

Highly Polarized Fermi Gases across a Narrow Feshbach Resonance

Ran Qi and Hui Zhai

Institute for Advanced Study, Tsinghua University, Beijing, 100084, China

(Dated: December 3, 2024)

We address the phase of highly polarized Fermi gases across a *narrow* Feshbach resonance starting from the problem of a single down spin fermion immersed in a Fermi sea of up spins. Both polaron and pairing states are considered using the variational wave function approach, and we find that the polaron to pairing transition will take place at the BCS side of the resonance, strongly in contrast to a wide resonance where the transition is located at the BEC side. For pairing phase, we find out the critical strength of repulsive interaction between pairs above which the mixture of pairs and fermions will not phase separate. Therefore, nearby a narrow resonance, it is quite likely that magnetism can coexist with *s*-wave BCS superfluidity at large Zeeman field, which is a remarkable property absent in conventional BCS superconductors (or fermion pair superfluids).

Whether an *s*-wave superconductor (or fermion pair superfluid) can coexist with magnetism is a long standing issue in condensed matter physics. Back to 1960s', Chandrasekhar and Clogston independently considered the response of a BCS superconductor to spin polarization due to a Zeeman field [1, 2]. They found that an *s*-wave superconductor will remain unpolarized until a critical Zeeman energy $h_c = \mu_\uparrow - \mu_\downarrow \sim \Delta/\sqrt{2}$, at which the system undergoes a sharp phase transition to a partially polarized normal state, and this critical field is now known as Chandrasekhar-Clogston (CC) limit of superconductor. In this scenario, superconductivity can not coexist with magnetism. Later on, there are several proposals for magnetized *s*-wave superconducting states, and the most famous ones are the Fulde-Ferrell-Larkin-Ovchinnikov state [3] and the Sarma State [4]. However, so far none of them have been firmly observed in an *s*-wave BCS superconductors.

In the last a few years, this problem has been revisited by a series of experiments on two-component Fermi gases with population imbalance [5–9]. Experiments have reached a consensus that at resonance regime and the BCS side, there is a CC limit, where a direct transition from a fully paired fermion superfluid to a partially polarized normal state has been observed, and no evidence of a magnetized superfluid has been found [5, 8–10]. However, all these studies were done across a wide resonance, where the resonance width is much larger than the Fermi energy. Recently, several experimental groups have begun to study narrow Feshbach resonances, such as ${}^6\text{Li}$ at 543.25G [11] or ${}^6\text{Li}$ - ${}^{40}\text{K}$ mixture at 154.719G [12], where the resonance width is comparable to Fermi energy, and therefore need to be considered. In this letter we find that the resonance width indeed has dramatic effect on physics of highly polarized Fermi gases.

In contrast to a wide resonance, to character a Fermi gas nearby a narrow resonance one not only needs $k_F a_s^0$, where a_s^0 is zero-energy scattering length between fermions, but also needs to consider $k_F/(W a_{bg})$ where W is the resonance width and a_{bg} is the background scattering length, and $k_F a_{bb}$ where a_{bb} is the scattering length

between closed channel molecules. In this work we focus on highly polarized limit and show all three parameters play important role in determining the nature of many-body phases. The studies of this work contain two part:

First, we consider a single down spin immersed in a Fermi sea of up spins. Two different types of states are compared, which are polaronic state and pairing state. For polaronic state, the single down spin is dressed by particle-hole pairs of up spins, and becomes a fermionic quasi-particle [13]. If this state has lower energy, the system will be a normal state of polaron Fermi liquid at sufficient high polarization. For the pairing state, one of the up spins will form a bound state with the single down spin. If this state has lower energy, each down spin will form a pair, and the system will be a mixture of condensed pairs and majority fermions. For wide resonance, a polaron to pairing transition takes place at the BEC side of the resonance [14–16]. Here we show that as the width of resonance gets narrower, the transition point will be shifted toward the BCS side. We find out how the critical value of $(k_F a_s^0)_c$ changes with the resonance width $k_F/(W a_{bg})$.

Secondly, when the pairing state has lower energy, the mixture of pairs and fermions may phase separate due to the repulsion between pairs and fermions. A strong enough repulsion between pairs are crucial to stabilize a uniform mixture. For a given $k_F/(W a_{bg})$, we find out the critical repulsion $(k_F a_{bb})_c$ as a function of $k_F a_s^0$.

Hence, we conclude that when $1/(k_F a_s^0) > 1/(k_F a_s^0)_c$ and $k_F a_{bb} > (k_F a_{bb})_c$, it is energetically favorable for minority fermions to form pairs, and condensate of fermion pairs can uniformly mixed with majority fermions, that is to say, magnetism can coexist with fermion pair superfluids at high polarized Fermi gas. The fact that this can happen at the BCS side and resonance regime represents a significant distinction between narrow and wide resonance. As the response to spin polarization is concerned, at resonance, or even at the BCS side, this system behaves similar as the BEC side of a wide resonance. This picture is also consistent with a recent high-temperature study of narrow resonance [17].

Model: We use the following two-channel model $\hat{H} = \hat{H}_0 + \hat{V}_c + \hat{V}_{bg} + \hat{V}_{bb}$ to describe a narrow resonance

$$\hat{H}_0 = \sum_{\mathbf{k}} (\epsilon_{\mathbf{k}}^b + \nu_0) b_{\mathbf{k}}^\dagger b_{\mathbf{k}} + \sum_{\mathbf{k}} (\epsilon_{\mathbf{k}}^u u_{\mathbf{k}}^\dagger u_{\mathbf{k}} + \epsilon_{\mathbf{k}}^d d_{\mathbf{k}}^\dagger d_{\mathbf{k}}) \quad (1)$$

$$\hat{V}_c = g_0 \sum_{\mathbf{k}\mathbf{q}} \Lambda_{\mathbf{k}} (b_{\mathbf{q}}^\dagger d_{\mathbf{q}-\mathbf{k}} u_{\mathbf{k}} + u_{\mathbf{k}}^\dagger d_{\mathbf{q}-\mathbf{k}}^\dagger b_{\mathbf{q}}) \quad (2)$$

$$\hat{V}_{bg} = U_0 \sum_{\mathbf{k}\mathbf{k}'\mathbf{q}} \Lambda_{\mathbf{k}} \Lambda_{\mathbf{k}'} u_{\mathbf{k}}^\dagger d_{\mathbf{q}-\mathbf{k}}^\dagger d_{\mathbf{q}-\mathbf{k}'} u_{\mathbf{k}'} \quad (3)$$

$$\hat{V}_{bb} = U_{bb} \sum_{\mathbf{k}\mathbf{k}'\mathbf{q}} b_{\mathbf{k}}^\dagger b_{\mathbf{q}-\mathbf{k}}^\dagger b_{\mathbf{q}-\mathbf{k}'} b_{\mathbf{k}'} \quad (4)$$

where u^\dagger and d^\dagger are creation operators for majority up spin and minority down spin, respectively, and b^\dagger is creation operator for bosonic closed channel molecule. $\epsilon_{\mathbf{k}}^b = \hbar^2 \mathbf{k}^2 / (2(m^u + m^d))$, and $\epsilon_{\mathbf{k}}^{u/d} = \hbar^2 \mathbf{k}^2 / (2m^{u/d})$. $\gamma = m_d/m_u$ is the mass ratio. \hat{V}_c and \hat{V}_{bg} represent the inter-channel coupling and the background scattering, respectively. $\Lambda_{\mathbf{k}} = \Theta(\Lambda - |\mathbf{k}|)$ and Λ is the momentum cut-off. In the Hamiltonian, the molecule detuning ν_0 , the inter-channel coupling g_0 and the background interaction parameter U_0 are bare quantities with Λ dependence, which need to be renormalized as follows [18]: $\nu_0(\Lambda) = \nu_r - [1 - Z(\Lambda)]g_r^2/U_r$, $g_0(\Lambda) = Z(\Lambda)g_r$, and $U_0(\Lambda) = Z(\Lambda)U_r$, where $Z(\Lambda) = (1 - U_r m_r \Lambda / \pi^2)^{-1}$, $1/m_r = 1/m^u + 1/m^d$ and $U_r = 2\pi a_{bg}/m_r$. The renormalized quantities U_r , g_r and ν_r are related to a_s as

$$\frac{2\pi a_s(E)}{m_r} = \left[\left(U_0 + \frac{g_0^2}{E - \nu_0} \right)^{-1} + \frac{m_r \Lambda}{\pi^2} \right]^{-1} = U_r + \frac{g_r^2}{E - \nu_r}$$

and the zero-energy scattering length a_s^0 is given by $a_s^0 = m_r(U_r - g_r^2/\nu_r)/2\pi$. Denoting $\nu_r = \Delta\mu(B - B_0)$, where B_0 is the location of the resonance and $\Delta\mu$ is the difference of magnetic moment between two channels, and introducing $W = g_r^2/U_r$, we have $a_s^0 = a_{bg}[1 - W/(\Delta\mu(B - B_0))]$, and $a_s(E) = a_{bg}[1 + W/(E - \Delta\mu(B - B_0))]$ where $W a_{bg}$ is always positive. For U_{bb} , since we only consider it to the mean-field order, we will take it as $U_{bb} = 4\pi\hbar^2 a_{bb}/(m_\uparrow + m_\downarrow)$. Our following results will be presented in terms of physical parameters (W , B_0 , $k_F a_s^0$, $k_F a_{bg}$ and $k_F a_{bb}$).

Polaronic State: We first adopt the following variational wave function which includes one particle-hole contribution

$$|\psi^P\rangle = \left[\phi_0 d_0^\dagger + \sum_{\mathbf{k}\mathbf{q}} \phi_{\mathbf{k}\mathbf{q}} u_{\mathbf{k}}^\dagger d_{\mathbf{q}-\mathbf{k}}^\dagger u_{\mathbf{q}} + \sum_{\mathbf{q}} \eta_{\mathbf{q}} b_{\mathbf{q}}^\dagger u_{\mathbf{q}} \right] |\text{FS}\rangle. \quad (5)$$

Here and below, all the summations with ' of \mathbf{k} and \mathbf{q} are restricted to $|\mathbf{k}| > k_F$ and $|\mathbf{q}| < k_F$, respectively. After energy minimization we obtain a self-consistent equation for polaron energy

$$E = \sum_{\mathbf{q}} \Gamma_2(\mathbf{q}, E + \epsilon_{\mathbf{q}}^u), \quad (6)$$

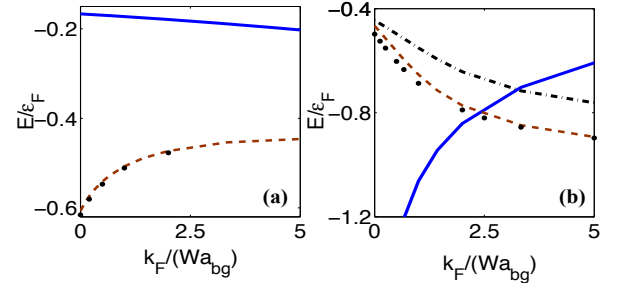


FIG. 1: Polaron energy as a function of $k_F/(W a_{bg})$. (a) $\gamma = 1$ and different interaction parameters. $1/(k_F a_s^0) = 0$ (dash line) and $1/(k_F a_s^0) = -2$ (solid line). (b) $1/(k_F a_s^0) = 0$ with different mass ratio. $\gamma = 6/40$ (solid line), $\gamma = 40/6$ (dash-dotted line) and $\gamma = \infty$ (dash line). All curves are results from one particle-hole approximation, while solid black dots are results including two particle-hole pairs contributions. $k_F a_{bg}$ is chosen as -0.1 .

where $\Gamma_2(\mathbf{q}, E + \epsilon_{\mathbf{q}}^u)$ coincides with two-particle vertex with total momentum \mathbf{q} and total energy $E + \epsilon_{\mathbf{q}}^u$ within the ladder approximation. This is because the variational wave function $|\psi^P\rangle$ describes the processes that an up spin (taken out from an occupied state \mathbf{q}) and the single down spin undergo repeated scattering, as well as coherent conversion between open and closed channels. This physical process is precisely what is captured by the ladder approximation.

The explicit form of $\Gamma_2(\mathbf{q}, E + \epsilon_{\mathbf{q}}^u)$ is given as

$$\Gamma_2(\mathbf{q}, E + \epsilon_{\mathbf{q}}^u) = \left[\frac{m_r}{2\pi a_s(E + \epsilon_{\mathbf{q}}^u - \epsilon_{\mathbf{q}}^b)} + I(\mathbf{q}, E + \epsilon_{\mathbf{q}}^u) \right]^{-1}, \quad (7)$$

where $I(\mathbf{q}, E + \epsilon_{\mathbf{q}}^u) = \sum_{\mathbf{k}}' 1/[\epsilon_{\mathbf{k}}^u + \epsilon_{\mathbf{q}-\mathbf{k}}^d - (E + \epsilon_{\mathbf{q}}^u)] - \sum_{\mathbf{k}} 1/(\epsilon_{\mathbf{k}}^u + \epsilon_{-\mathbf{k}}^d)$. The only difference between Eq. (7) and the previous results for a wide resonance [13, 14] is that a constant a_s is replaced by an energy dependent one $a_s(E + \epsilon_{\mathbf{q}}^u - \epsilon_{\mathbf{q}}^b)$, where $E + \epsilon_{\mathbf{q}}^u - \epsilon_{\mathbf{q}}^b$ represents the energy of relative motion for two atoms undergoing repeated scattering.

The polaron energy as a function of resonance width is plotted in Fig. (1) from solving self-consistency equation Eq. (6). As one can see, when the dimensionless parameter $k_F/(W a_{bg})$ increases from zero, (i) for $\gamma = 1$, and nearby resonance $1/(k_F a_s^0) \approx 0$ polaron energy E will increase, while at the BCS side $1/(k_F a_s^0) \ll 0$, E will decrease; and (ii) at resonance, if γ is greater than a critical value, E will also decrease. By analyzing energy dependence of a_s , we can qualitatively understand these behaviors as the width deviates from infinity. When \mathbf{q} varies from 0 to k_F , $E + \epsilon_{\mathbf{q}}^u - \epsilon_{\mathbf{q}}^b$ varies from E to $E + \gamma\epsilon_F/(1 + \gamma)$. For $\gamma = 1$, and since $E = -0.6\epsilon_F$ when $k_F/(W a_{bg}) = 0$, $E + \epsilon_{\mathbf{q}}^u - \epsilon_{\mathbf{q}}^b$ is always negative, and therefore $a_s(E + \epsilon_{\mathbf{q}}^u - \epsilon_{\mathbf{q}}^b)$ is also negative, which means effectively the interaction becomes less attractive, and therefore E increases. At the BCS side, when $E > -0.5\epsilon_F$, there will be both neg-

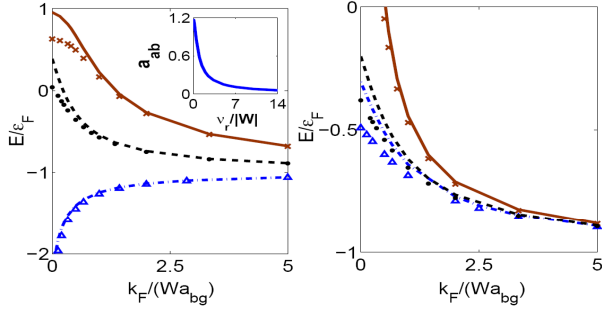


FIG. 2: Pairing state energy as a function of $k_F/(Wa_{bg})$. (a) mass ratio $\gamma = 1$ and different interaction parameters. $1/(k_F a_s^0) = 0$ (solid line), $1/(k_F a_s^0) = -1$ (dash line) and $1/(k_F a_s^0) = 1$ (dash-dotted line). (b) $1/(k_F a_s^0) = 0$ but different mass ratio. $\gamma = 6/40$ (solid line), $\gamma = 40/6$ (dash line) and $\gamma = \infty$ (dash-dotted line). All the curves are computed from bare pairs, while the dots, crosses and triangles are results with one particle-hole contributions. Inset of (a): the atom-dimer scattering length a_{ab} (in unit of $\sqrt{mE_b}/\hbar$) as a function of ν_r/W . $k_F a_{bg}$ is chosen as -0.1 .

ative contribution to $E + \epsilon_{\mathbf{q}}^u - \epsilon_{\mathbf{q}}^b$ from small \mathbf{q} and positive contributions from \mathbf{q} nearby k_F , while the later can easily become dominative due to the larger phase space. Hence, the interaction becomes effectively more attractive, and therefore E decreases. Similarly, if γ becomes larger, the polaron energy at $k_F/(Wa_{bg}) = 0$ increases at resonance, and $\gamma\epsilon_F/(1 + \gamma)$ also becomes larger. For same reason, for large enough γ , the contribution to $E + \epsilon_{\mathbf{q}}^u - \epsilon_{\mathbf{q}}^b$ will also be dominated by positive contributions nearby Fermi surface, and therefore E will decrease.

We have also checked the energy convergence by considering two particle-hole contributions [19, 20]. The numerical solutions with two particle-hole contributions are shown as the dots in Fig. (1). For $\gamma = 1$, one can see that the corrections from two particle-hole pairs are always negligible small, and it becomes even smaller as $|W|$ decreases. While for $\gamma \rightarrow \infty$, the deviation is a little larger (dashed line and the dots in (b)), as already noted in [19] for a wide resonance, but it is still within only a few percents. This result justifies the validity of the expansion in terms of the number of particle-hole pairs in computing energy for a narrow resonance.

Pairing State: For pairing state, we use the variational wave function first introduced in Ref. [14]:

$$|\psi^m\rangle = \left[\eta_0 b_0^\dagger + \sum_{\mathbf{k}} A_{\mathbf{k}} u_{\mathbf{k}}^\dagger d_{-\mathbf{k}}^\dagger + \sum_{\mathbf{k}\mathbf{q}} \phi_{\mathbf{k}\mathbf{q}} b_{\mathbf{q}-\mathbf{k}}^\dagger u_{\mathbf{k}}^\dagger u_{\mathbf{q}} + \sum_{\mathbf{k}'\mathbf{k}\mathbf{q}} \Phi_{\mathbf{k}\mathbf{k}'\mathbf{q}} u_{\mathbf{k}'}^\dagger d_{\mathbf{q}-\mathbf{k}-\mathbf{k}'}^\dagger u_{\mathbf{k}}^\dagger u_{\mathbf{q}} \right] |\text{FS}\rangle \quad (8)$$

If we only consider bare pair wave function without including particle-hole contribution, the pair state energy is given by $\Gamma_2^{-1}(0, E + \epsilon_F) = 0$, as shown in the lines of Fig. (2). The interaction between pair and majority up spins

can be described by including particle-hole pairs. Up to one particle-hole pair, by minimizing energy we obtain a closed integral equation for $\eta_{\mathbf{k}\mathbf{q}} = 2U_0 \sum_{\mathbf{p}} \Lambda_{\mathbf{p}} \Phi_{\mathbf{k}\mathbf{p}\mathbf{q}}$:

$$\sum_{\mathbf{q}'} \frac{\eta_{\mathbf{k}\mathbf{q}'}}{E_{\mathbf{k}}} - \sum_{\mathbf{k}'\mathbf{q}'} \frac{\eta_{\mathbf{k}'\mathbf{q}'}}{\gamma_E E_{\mathbf{k}} E_{\mathbf{k}'}} - \sum_{\mathbf{k}'} \frac{\eta_{\mathbf{k}'\mathbf{q}}}{E_{\mathbf{k}\mathbf{k}'\mathbf{q}}} + \gamma_{\mathbf{k}\mathbf{q}} \eta_{\mathbf{k}\mathbf{q}} = 0 \quad (9)$$

where $E_{\mathbf{k}} = \epsilon_{\mathbf{k}}^u + \epsilon_{\mathbf{k}}^d - E - \epsilon_F$, $E_{\mathbf{k}\mathbf{k}'\mathbf{q}} = \epsilon_{\mathbf{k}'}^u + \epsilon_{\mathbf{k}}^u + \epsilon_{\mathbf{q}-\mathbf{k}-\mathbf{k}'}^d - \epsilon_{\mathbf{k}}^u - E - \epsilon_F$ and $\gamma_{\mathbf{k}\mathbf{q}} = \Gamma_2^{-1}(\mathbf{q} - \mathbf{k}, E + \epsilon_F + \epsilon_{\mathbf{q}}^u - \epsilon_{\mathbf{k}}^u)$, $\gamma_E = \Gamma_2^{-1}(0, E + \epsilon_F)$. The numerical solution of these equations are also shown in Fig. (2). We find that as $k_F/(Wa_{bg})$ increases, the pairing state energy decreases at the BCS side and at resonance regime, despite of different mass ratios; while it increases at the BEC side. This can be explained by similar argument of energy dependence of $a_s(E)$ as made for polaron above. An important feature one can find from Fig. (2) is that in the limit $W \rightarrow 0$, the pairing state energy always saturates to $-\epsilon_F$. This can be understood as follows: when one down spin is added into the system, an up spin is taken out from the Fermi sea (subtract energy ϵ_F) to form a pair with the down spin, whose energy approaches ν_r in the limit $W \rightarrow 0$. Thus the pairing state energy should approach $-\epsilon_F + \nu_r$ [21]. Moreover, at resonance, $\nu_r = 0$. Away from resonance, if one fixes a_s^0 and take the infinite narrow limit $W \rightarrow 0$, ν_r should also approach zero with a fixed ratio W/ν_r . Hence the pairing state energy always approaches $-\epsilon_F$. In fact, this also indicates that the interaction between a pair and the residual majority atoms vanishes in the limit

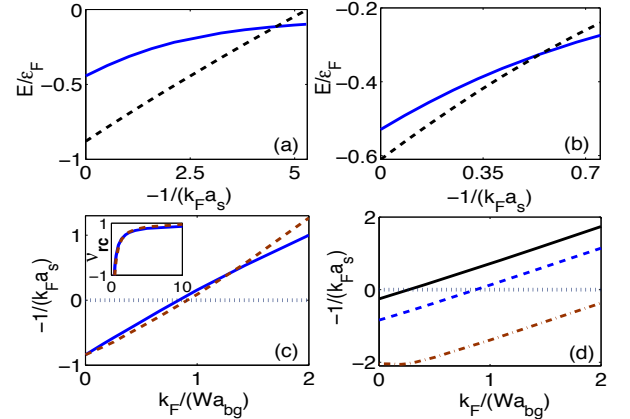


FIG. 3: (a-b) Polaron energy (solid line), pairing state energy (dash line) as a function of magnetic field for ${}^6\text{Li}$ (a) and ${}^6\text{Li}$ - ${}^{40}\text{K}$ mixture (b). For (a), we take $k_F a_{bg} = 0.016$ and $W = 12.2\epsilon_F$ [11], and for (b) we take $k_F a_{bg} = 0.022$ and $W = 54.91\epsilon_F$ [23]. In (b), ${}^{40}\text{K}$ is taken as minority component. (c-d) The critical value of the transition $1/(k_F a_s^0)_c$ as a function of $k_F/(Wa_{bg})$. For (c), $\gamma = 1$ but different $k_F a_{bg}$. $k_F a_{bg} = -0.1$ (solid line) and $k_F a_{bg} = 0.1$ (dashed line). For (d), $k_F a_{bg} = 0.01$ but different γ . $\gamma = 40/6$ (solid line), $\gamma = 1$ (dash line) and $\gamma = 6/40$ (dash-dotted line). Inset of (c), the critical value of transition in term of ν_r^c (in unit of ϵ_F) as a function of $k_F/(Wa_{bg})$.

$W \rightarrow 0$. We have performed a three-body calculation and find out the atom-dimer scattering length a_{ab} from the asymptotic behavior of the three-body wave function [20, 22], as shown in the inset of Fig. (2)(a), which indeed shows $a_{ab} \rightarrow 0$ as $W \rightarrow 0$.

Polaron-Pairing Transition: The transition from polaronic state to pairing state can now be determined by comparing their energies. In Fig. (3)(a-b) we consider two concrete samples studied in current experiments: ${}^6\text{Li}$ at 543.25G and ${}^6\text{Li}$ - ${}^{40}\text{K}$ mixture at 154.719 G, and the parameters are typical values taken from experimental papers [11, 12, 23]. We found that in both cases, the polaron to pairing transition is located at the BCS side of the resonance, which is away from resonance with $\Delta\mu(B - B_0)$ on the order of ϵ_F . At the transition points, $1/(k_F a_s^0) = -4.35$ for ${}^6\text{Li}$ and $1/(k_F a_s^0) = -0.55$ for ${}^6\text{Li}$ - ${}^{40}\text{K}$ mixture, where the systems are very BCS-like. This transition can be experimentally observed by radio-frequency spectroscopy, as already done in a wide resonance [16].

In Fig. 3(c-d), we plot the critical value $1/(k_F a_s^0)$ for polaron to pairing transition as a function of resonance width $k_F/(W a_{bg})$. One find that when $k_F/(W a_{bg}) \gtrsim 1$, the transition will be shifted to the BCS side. This condition is equivalent to $|W|/\epsilon_F \lesssim 1/|k_F a_{bg}|$. Since usually $k_F a_{bg} \ll 1$, it means that the resonance width does not need to be very narrow. One also notes that the transition point is not sensitive to the value of $k_F a_{bg}$ itself (Fig. (3)(c)), but is sensitive to mass ratio (Fig. 3(d)). The inset of Fig. (3)(c) shows that in the limit $W \rightarrow 0$, the critical point will approach $\nu_r^c \rightarrow \epsilon_F$, which means that the pairing state will be favored once the energy of close channel molecule is below the Fermi energy.

Stability of the Mixture: For very low density of down spins and sufficiently narrow resonance, we can expand the equation-of-state in terms of the density of bosonic pairs n_b up to the second order [24]

$$\mathcal{E} = \mathcal{E}_F + \mu_b^0 n_b + \frac{1}{2} g n_b^2 \quad (10)$$

where \mathcal{E}_F is the energy density of spin- \uparrow Fermi sea, $\mu_b^0 = E + \epsilon_F$ where E is the pairing state energy computed above. The repulsion $g = \frac{4\pi\hbar^2}{m_\uparrow + m_\downarrow} a_{bb} + g_{\text{ind}}$ contains the contribution from bare interaction between closed channel molecules and the induced interactions g_{ind} from the interchannel coupling, which is calculated within Born approximation [20]. From Eq. (10) we obtain:

$$\mu_b = \frac{\partial \mathcal{E}}{\partial n_b} = \mu_b^0 + g n_b \quad (11)$$

$$\mu_\uparrow = \frac{\partial \mathcal{E}}{\partial n_\uparrow} = \epsilon_F + \frac{\partial \mu_b^0}{\partial n_\uparrow} n_b + O(n_b^2) \quad (12)$$

The stability condition against phase separation is given by $\frac{\partial \mu_\uparrow}{\partial n_\uparrow} \frac{\partial \mu_b}{\partial n_b} - \frac{\partial \mu_\uparrow}{\partial n_b} \frac{\partial \mu_b}{\partial n_\uparrow} > 0$ [25], from which we can determine the critical value for a_{bb} . The results are plotted in Fig. 4 for ${}^6\text{Li}$ (a) and ${}^6\text{Li}$ - ${}^{40}\text{K}$ (b) mixture in

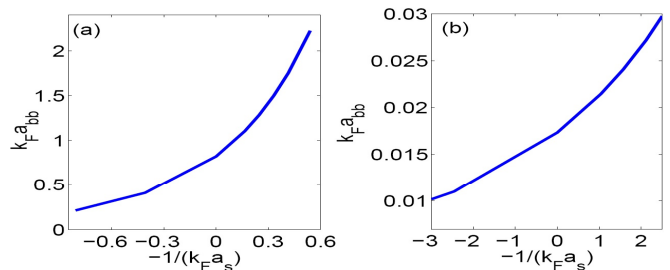


FIG. 4: The critical value required for $k_F a_{bb}$ to prevent phase separation as a function of $1/(k_F a_s^0)$, for ${}^6\text{Li}$ (a) and ${}^6\text{Li}$ - ${}^{40}\text{K}$ mixture (b), respectively.

the regime where pairing state is favorable. We can see that it requires $k_F a_{bb} > 0.017$ for ${}^6\text{Li}$ at resonance, and $k_F a_{bb} > 0.81$ for ${}^6\text{Li}$ - ${}^{40}\text{K}$ mixture at resonance. Very likely, this condition can be satisfied in ${}^6\text{Li}$ but not in ${}^6\text{Li}$ - ${}^{40}\text{K}$ mixture.

Acknowledgements. We thank Xiaoling Cui and Zeng-Qiang Yu for helpful discussions. This work is supported by Tsinghua University Initiative Scientific Research Program. HZ is supported by NSFC under Grant No. 11004118 and No. 11174176, and NKBRSCF under Grant No. 2011CB921500. RQ is supported by NSFC under Grant No. 11104157.

Note Added: As we are finishing writing the paper, we become aware of the experimental work from Innsbruck group in which the polaron to pairing transition has been observed in the BCS side [23]. This data is consistent with our theoretical results very well.

-
- [1] A. M. Glogston, Phys. Rev. Lett. **9**, 266 (1962).
 - [2] B. S. Chandrasekhar, Appl. Phys. Lett. **1**, 7 (1962).
 - [3] P. Fulde and R. A. Ferrell, Phys. Rev. **135**, A550 (1964); A. I. Larkin and Y. N. Ovchinnikov, Zh. Eksp. Teor. Fiz. **47**, 1136 (1964).
 - [4] G. Sarma, J. Phys. Chem. Solids. **24** 1029 (1963).
 - [5] M. W. Zwierlein, A. Schirotzek, C. H. Schunck, and W. Ketterle, Science **311**, 492 (2006); Y. Shin, M. W. Zwierlein, C. H. Schunck, A. Schirotzek, and W. Ketterle, Phys. Rev. Lett. **97**, 030401 (2006); Y. Shin, C. H. Schunck, A. Schirotzek, and W. Ketterle, Nature **451**, 689 (2008).
 - [6] Y. Shin, A. Schirotzek, C. H. Schunck and W. Ketterle, Phys. Rev. Lett. **101**, 070404 (2008).
 - [7] G. B. Partridge, W. Li, R. I. Kamar, Y. A. Liao, and R. G. Hulet, Science **311**, 503 (2006); G. B. Partridge *et al.*, Phys. Rev. Lett. **97**, 190407 (2006).
 - [8] S. Nascimbene, N. Navon, K. Jiang, L. Tarruell, M. Teichmann, J. McKeever, F. Chevy, C. Salomon, Phys. Rev. Lett. **103**, 18 (2009); S. Nascimbene N. Navon, K. Jiang, F. Chevy, C. Salomon, Nature **463**, 1057 (2010); and N. Navon, S. Nascimbene, F. Chevy, C. Salomon, Science **328**, 729 (2010); and S. Nascimbene, N. Navon, S. Pilati, F. Chevy, S. Giorgini, A. Georges, C. Salomon, Phys.

- Rev. Lett. **106** 215303 (2011)
- [9] Y. A. Liao, M. Reville, T. Paprotta, A. S. C. Rittner, W. Li, G. B. Partridge, R. G. Hulet, Phys. Rev. Lett. **107**, 145305 (2011)
- [10] F. Chevy and C. Mora, Rep. on Prog. in Phys. **73**, 112401 (2010); L. Radzihovsky and D. E. Sheehy, Rep. Prog. Phys. **73**, 076501 (2010).
- [11] K. E. Strecker, G. B. Partridge, and R. G. Hulet, Phys. Rev. Lett. **91**, 080406 (2003). K. O'Hara, presentation in Aspen, June, 2011.
- [12] A. Trenkwalder *et al.*, Phys. Rev. Lett. **106**, 115304 (2011).
- [13] F. Chevy, Phys. Rev. A **74**, 063628 (2006); R. Combescot, A. Recati, C. Lobo, and F. Chevy, Phys. Rev. Lett. **98**, 180402 (2007).
- [14] M. Punk, P. T. Dumitrescu, and W. Zwerger, Phys. Rev. A **80**, 053605 (2009).
- [15] N. V. Prokof'v and B. V. Svistunov, Phys. Rev. B **77**, 020408(R) (2008).
- [16] A. Schirotzek, C. H. Wu, A. Sommer, and M. W. Zwierlein, Phys. Rev. Lett. **102**, 230402 (2009).
- [17] Tin-Lun Ho and Xiaoling Cui, arXiv: 1105.4627 (2011).
- [18] S. Kokkelmans, J. Milstein, M. Chiofalo, R. Walser, and M. Holland, Phys. Rev. A **65**, 053617 (2002).
- [19] R. Combescot and S. Giraud, Phys. Rev. Lett. **101**, 050404 (2008).
- [20] The details are shown in the supplementary material.
- [21] D. E. Sheehy and L. Radzihovsky, Ann. Phys. **322**, 1790 (2007).
- [22] D. S. Petrov, Phys. Rev. A **67**, 010703(R) (2003).
- [23] C. Kohstall, M. Zaccanti, M. Jag, A. Trenkwalder, P. Massignan, G. M. Bruun, F. Schreck, R. Grimm, arXiv: 1112.0020
- [24] This expansion of energy functional is only valid for sufficiently narrow resonance where closed channel molecule is dominant in the pairing state.
- [25] L. Viverit, C. J. Pethick and H. Smith, Phys. Rev. A **61**, 053605 (2000); M. Iskin and C. A. R. Sa de Melo, Phys. Rev. A **77**, 013625 (2008).

SUPPLEMENTARY MATERIAL

Polaron energy including two particle-hole contributions

In this section of supplementary material, we derive the self-consistent equation for polaron energy including two particle-hole excitations.

The Hamiltonian under consideration is given as equation (1)-(3) in our paper, and the variational wave function is written as:

$$|\psi\rangle = |\hat{\phi}_0\rangle + |\hat{\phi}_{\mathbf{k}\mathbf{q}}\rangle + |\hat{\eta}_{\mathbf{q}}\rangle + |\hat{\alpha}\rangle + |\hat{\beta}\rangle \quad (13)$$

$$|\hat{\phi}_0\rangle = \phi_0 d_0^\dagger |FS\rangle, \quad |\hat{\phi}_{\mathbf{k}\mathbf{q}}\rangle = \sum_{\mathbf{k}\mathbf{q}}' \phi_{\mathbf{k}\mathbf{q}} u_{\mathbf{k}}^\dagger d_{\mathbf{q}-\mathbf{k}}^\dagger u_{\mathbf{q}} |FS\rangle, \quad |\hat{\eta}_{\mathbf{q}}\rangle = \sum_{\mathbf{q}}' \eta_{\mathbf{q}} b_{\mathbf{q}}^\dagger u_{\mathbf{q}} |FS\rangle \quad (14)$$

$$|\hat{\alpha}\rangle = \sum_{\mathbf{k}\mathbf{k}'\mathbf{q}\mathbf{q}}' \alpha_{\mathbf{k}\mathbf{k}'\mathbf{q}\mathbf{q}} u_{\mathbf{k}}^\dagger u_{\mathbf{k}'}^\dagger d_{\mathbf{q}+\mathbf{q}'-\mathbf{k}-\mathbf{k}'}^\dagger u_{\mathbf{q}} u_{\mathbf{q}'} |FS\rangle, \quad |\hat{\beta}\rangle = \sum_{\mathbf{k}\mathbf{q}\mathbf{q}}' \beta_{\mathbf{k}\mathbf{q}\mathbf{q}} b_{\mathbf{q}+\mathbf{q}'}^\dagger u_{\mathbf{k}}^\dagger u_{\mathbf{q}} u_{\mathbf{q}'} |FS\rangle \quad (15)$$

where $|FS\rangle$ is the Fermi sea of N spin- \uparrow particles, $|\hat{\phi}_{\mathbf{k}\mathbf{q}}\rangle$ and $|\hat{\eta}_{\mathbf{q}}\rangle$ correspond to single particle-hole excitation while $|\hat{\alpha}\rangle$, $|\hat{\beta}\rangle$ represents the contribution from two particle-hole excitation. All momentum summations are restricted within $|\mathbf{q}| < k_F$, $|\mathbf{k}| > k_F$ as mentioned in our paper. Now we solve the Schrödinger equation $\hat{H}|\psi\rangle = E|\psi\rangle$ and drop all the terms beyond two particle-hole excitation, we get the following set of equations:

$$E\phi_0 = \sum_{\mathbf{q}}' \varphi_{\mathbf{q}} \quad (16)$$

$$E_{\mathbf{k}\mathbf{q}}\phi_{\mathbf{k}\mathbf{q}} = -g_0\eta_{\mathbf{q}} - U_0\phi_0 - \varphi_{\mathbf{q}} + \sum_{\mathbf{q}'}' G_{\mathbf{k}\mathbf{q}\mathbf{q}'} \quad (17)$$

$$E_{\mathbf{q}}\eta_{\mathbf{q}} = \frac{g_0}{U_0}\varphi_{\mathbf{q}} \quad (18)$$

$$E_{\mathbf{k}\mathbf{k}'\mathbf{q}\mathbf{q}'}4\alpha_{\mathbf{k}\mathbf{k}'\mathbf{q}\mathbf{q}'} = 2g_0(\Lambda_{\mathbf{k}'}\beta_{\mathbf{k}\mathbf{q}\mathbf{q}'} - \Lambda_{\mathbf{k}}\beta_{\mathbf{k}'\mathbf{q}\mathbf{q}'} + U_0[(\phi_{\mathbf{k}\mathbf{q}} - \phi_{\mathbf{k}\mathbf{q}'}) - (\phi_{\mathbf{k}'\mathbf{q}} - \phi_{\mathbf{k}'\mathbf{q}'})] - G_{\mathbf{k}\mathbf{q}\mathbf{q}'} + G_{\mathbf{k}'\mathbf{q}\mathbf{q}'} \quad (19)$$

$$E_{\mathbf{k}\mathbf{q}\mathbf{q}'}\beta_{\mathbf{k}\mathbf{q}\mathbf{q}'} = -\frac{g_0}{2U_0}G_{\mathbf{k}\mathbf{q}\mathbf{q}'} \quad (20)$$

where $\varphi_{\mathbf{q}} = U_0 \sum_{\mathbf{k}}' \phi_{\mathbf{k}\mathbf{q}}$, $G_{\mathbf{k}\mathbf{q}\mathbf{q}'} = 4U_0 \sum_{\mathbf{K}}' \alpha_{\mathbf{k}\mathbf{K}\mathbf{q}\mathbf{q}'}$ and we have defined:

$$\begin{aligned} E_{\mathbf{q}} &= E + \epsilon_{\mathbf{q}}^u - \epsilon_{\mathbf{q}}^b - \nu_0 & E_{\mathbf{k}\mathbf{q}} &= \epsilon_{\mathbf{k}}^u + \epsilon_{\mathbf{q}-\mathbf{k}}^d - \epsilon_{\mathbf{q}}^u - E \\ E_{\mathbf{k}\mathbf{q}\mathbf{q}'} &= E + \epsilon_{\mathbf{q}}^u + \epsilon_{\mathbf{q}'}^u - \epsilon_{\mathbf{k}}^u - \epsilon_{\mathbf{q}+\mathbf{q}'-\mathbf{k}}^b - \nu_0 & E_{\mathbf{k}\mathbf{k}'\mathbf{q}\mathbf{q}'} &= \epsilon_{\mathbf{k}}^u + \epsilon_{\mathbf{k}'}^u + \epsilon_{\mathbf{q}+\mathbf{q}'-\mathbf{k}-\mathbf{k}'}^d - \epsilon_{\mathbf{q}}^u - \epsilon_{\mathbf{q}'}^u - E \end{aligned}$$

Finally, after eliminating all the variables other than $G_{\mathbf{k}\mathbf{q}\mathbf{q}'}$ from equation (16)-(20) and using the renormalization relations between U_0 , g_0 , ν_0 and U_r , g_r , ν_r as given in our paper, we obtain the following integral equations:

$$E = \sum_{\mathbf{q}} \Gamma_2^{-1}(\mathbf{q}, E + \epsilon_{\mathbf{q}}^u) \left(1 + \sum_{\mathbf{k}\mathbf{q}'} G_{\mathbf{k}\mathbf{q}\mathbf{q}'}/E_{\mathbf{k}\mathbf{q}} \right), \quad (21)$$

$$\gamma_{\mathbf{k}\mathbf{q}\mathbf{q}'} G_{\mathbf{k}\mathbf{q}\mathbf{q}'} = \phi_{\mathbf{k}\mathbf{q}'} - \phi_{\mathbf{k}\mathbf{q}} + \sum_{\mathbf{k}'} G_{\mathbf{k}'\mathbf{q}\mathbf{q}'}/E_{\mathbf{k}\mathbf{k}'\mathbf{q}\mathbf{q}'}, \quad (22)$$

$$\phi_{\mathbf{k}\mathbf{q}} = \frac{1}{E_{\mathbf{k}\mathbf{q}}} \left[\sum_{\mathbf{q}'} G_{\mathbf{k}\mathbf{q}\mathbf{q}'} - \Gamma_2^{-1}(\mathbf{q}, E + \epsilon_{\mathbf{q}}^u) \left(1 + \sum_{\mathbf{k}'\mathbf{q}'} \frac{G_{\mathbf{k}'\mathbf{q}\mathbf{q}'}}{E_{\mathbf{k}'\mathbf{q}}} \right) \right], \quad (23)$$

where $\gamma_{\mathbf{k}\mathbf{q}\mathbf{q}'} = \Gamma_2^{-1}(\mathbf{q} + \mathbf{q}' - \mathbf{k}, E + \epsilon_{\mathbf{q}}^u + \epsilon_{\mathbf{q}'}^u - \epsilon_{\mathbf{k}}^u)$, $E_{\mathbf{k}\mathbf{q}} = \epsilon_{\mathbf{k}}^u + \epsilon_{\mathbf{q}-\mathbf{k}}^d - \epsilon_{\mathbf{q}}^u - E$ and $E_{\mathbf{k}\mathbf{k}'\mathbf{q}\mathbf{q}'} = \epsilon_{\mathbf{k}}^u + \epsilon_{\mathbf{k}'}^u + \epsilon_{\mathbf{q}+\mathbf{q}'-\mathbf{k}-\mathbf{k}'}^d - \epsilon_{\mathbf{q}}^u - \epsilon_{\mathbf{q}'}^u - E$. Γ_2^{-1} has been defined in equation (6) in our paper. The above integral equations are solved by numeric iterations to obtain the polaron energy E .

Three-body problem and the atom-dimer scattering length

In this section of supplementary material we obtain the atom-molecule scattering length by solving the three-body problem using a two-channel model (see equation (1)-(3) in our paper). We first write the three-body wave function in the following second quantized form in momentum space:

$$|\psi_3\rangle = \left[\sum_{\mathbf{k}_1\mathbf{k}_2} \phi_{\mathbf{k}_1\mathbf{k}_2} u_{\mathbf{k}_1}^\dagger u_{\mathbf{k}_2}^\dagger d_{-\mathbf{k}_1-\mathbf{k}_2}^\dagger + \sum_{\mathbf{p}} \eta_{\mathbf{p}} u_{\mathbf{p}}^\dagger b_{-\mathbf{p}}^\dagger \right] |\text{vac}\rangle \quad (24)$$

From the Schrödinger equation $\hat{H}|\psi_3\rangle = E|\psi_3\rangle$, we have:

$$(\epsilon_{\mathbf{k}}^u + \epsilon_{\mathbf{k}'}^u + \epsilon_{\mathbf{k}+\mathbf{k}'}^d - E)\phi_{\mathbf{k}\mathbf{k}'} + U_0 \sum_{\mathbf{p}} (\phi_{\mathbf{p}\mathbf{k}'} - \phi_{\mathbf{p}\mathbf{k}}) + \frac{1}{2}g_0(\eta_{\mathbf{k}'} - \eta_{\mathbf{k}}) = 0 \quad (25)$$

$$(\epsilon_{\mathbf{k}}^u + \epsilon_{\mathbf{k}}^b + \nu_0 - E)\eta_{\mathbf{k}} + 2g_0 \sum_{\mathbf{k}'} \phi_{\mathbf{k}'\mathbf{k}} = 0 \quad (26)$$

Defining $\alpha_{\mathbf{k}} = U_0 \sum_{\mathbf{k}'} \phi_{\mathbf{k}'\mathbf{k}}$ and using the renormalization relation (here the introducing of the prefactor U_0 is just to eliminate the ultra-violet divergence in $\sum_{\mathbf{k}'}$, this divergence corresponds to the $\frac{1}{r}$ singularity in the real space wave function), we have:

$$\gamma_{\mathbf{k}}\alpha_{\mathbf{k}} = \sum_{\mathbf{k}'} \frac{\alpha_{\mathbf{k}'}}{E_{\mathbf{k}'\mathbf{k}}} \quad (27)$$

$$\eta_{\mathbf{k}} = \frac{2g_r}{U_r} \frac{\alpha_{\mathbf{k}}}{E_{\mathbf{k}}} \quad (28)$$

where $E_{\mathbf{k}} = E - \epsilon_{\mathbf{k}}^u - \epsilon_{\mathbf{k}}^b - \nu_0$, $E_{\mathbf{k}'\mathbf{k}} = \epsilon_{\mathbf{k}}^u + \epsilon_{\mathbf{k}'}^u + \epsilon_{\mathbf{k}+\mathbf{k}'}^d - E$ and we define:

$$\gamma_{\mathbf{k}} = \left(U_r + \frac{g_r^2}{E - \epsilon_{\mathbf{k}}^u - \epsilon_{\mathbf{k}}^b - \nu_r} \right)^{-1} + \sum_{\mathbf{k}'} \left(\frac{1}{E_{\mathbf{k}\mathbf{k}'}} - \frac{1}{\epsilon_{\mathbf{k}'}^r} \right) \quad (29)$$

The fourier transform $\alpha(\mathbf{r}) = (2\pi)^3 \int d^3\mathbf{k} \alpha_{\mathbf{k}} e^{i\mathbf{k}\cdot\mathbf{r}}$ is just the asymptotic wave function between an atom and a molecule. To see this, we first write wave function (24) in real space:

$$|\psi_{3b}\rangle = \int d^3\mathbf{r}_1 d^3\mathbf{r}_2 d^3\mathbf{r}_3 \left[\phi_o(\mathbf{r}_1, \mathbf{r}_2, \mathbf{r}_3) u^\dagger(\mathbf{r}_1) u^\dagger(\mathbf{r}_2) d^\dagger(\mathbf{r}_3) + \phi_c(\mathbf{r}_1, \mathbf{r}_2, \mathbf{r}_3) u^\dagger(\mathbf{r}_1) b^\dagger(\mathbf{r}_3) \right] |\text{vac}\rangle \quad (30)$$

$$\phi_o(\mathbf{r}_1, \mathbf{r}_2, \mathbf{r}_3) = \sum_{\mathbf{k}_1\mathbf{k}_2} \phi_{\mathbf{k}_1\mathbf{k}_2} e^{i\mathbf{k}_1\cdot(\mathbf{r}_1-\mathbf{r}_3)} e^{i\mathbf{k}_2\cdot(\mathbf{r}_2-\mathbf{r}_3)} \quad (31)$$

$$\phi_c(\mathbf{r}_1, \mathbf{r}_2, \mathbf{r}_3) = \delta^3(\mathbf{r}_2 - \mathbf{r}_3) \sum_{\mathbf{p}} \eta_{\mathbf{p}} e^{i\mathbf{p}\cdot(\mathbf{r}_1-\mathbf{r}_3)} = \delta^3(\mathbf{r}_2 - \mathbf{r}_3) \eta(\mathbf{r}_1 - \mathbf{r}_3) \quad (32)$$

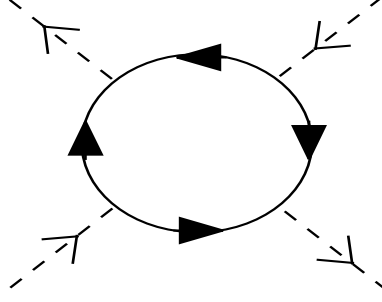


FIG. 5: Induced molecule-molecule interaction under Born approximation. The dashed and solid line refers to the propagator of molecule and atoms respectively. Each vertex is given by the inter-channel coupling g_r .

In the limit $\mathbf{r}_2 - \mathbf{r}_3 \rightarrow 0$, we have $\phi_o(\mathbf{r}_1, \mathbf{r}_2, \mathbf{r}_3) \simeq \sum_{\mathbf{k}_1} (\sum_{\mathbf{k}_2} \phi_{\mathbf{k}_1 \mathbf{k}_2}) e^{i\mathbf{k}_1 \cdot (\mathbf{r}_1 - \mathbf{r}_3)} = \frac{1}{U_0} \alpha(\mathbf{r}_1 - \mathbf{r}_3)$ and $\phi_c(\mathbf{r}_1, \mathbf{r}_2, \mathbf{r}_3) = \delta^3(\mathbf{r}_2 - \mathbf{r}_3) \eta(\mathbf{r}_1 - \mathbf{r}_3)$. On the other hand, from equation (28) we can see that $\eta_{\mathbf{k}}$ and $\alpha_{\mathbf{k}}$ has identical singularity as $k \rightarrow 0$ (since $\frac{1}{E_{\mathbf{k}}}$ is analytical near $k = 0$). This means that in real space, $\eta(\mathbf{r})$ and $\alpha(\mathbf{r})$ have the same long range behavior as $r \rightarrow \infty$. As a result, the long range behavior of $\alpha(\mathbf{r})$ represents the asymptotic wave function between an atom and a molecule as they separate far away from each other.

As $r \rightarrow \infty$, we have $\alpha(\mathbf{r}) = 1 - \frac{a_{am}}{r} (1 + O(r^{-1}))$ where a_{am} is the atom-molecule scattering length. This leads to the fact that $\alpha_{\mathbf{k}} = \delta^3(\mathbf{k}) - \frac{1}{2\pi^2} \frac{a_{am}}{k^2} (1 + O(k))$ as $k \rightarrow 0$. As a result, it will be very convenient to define $\alpha_{\mathbf{k}} = \delta^3(\mathbf{k}) - \frac{1}{2\pi^2} \frac{\beta_{\mathbf{k}}}{k^2}$ and we have:

$$\beta_{\mathbf{k}} = \frac{-k^2}{4\pi\gamma_{\mathbf{k}}} \left[\frac{1}{E_{0\mathbf{k}}} - 4\pi \int \frac{d^3\mathbf{q}}{8\pi^3} \frac{\beta_{\mathbf{q}}}{q^2 E_{\mathbf{q}\mathbf{k}}} \right] \quad (33)$$

The above integral equation is solved numerically and the atom-molecule scattering length is given as $a_{am} = \beta_0$.

Induced Interaction

In this section of supplementary material, we evaluate the induced interaction g_{ind} within Born approximation. The corresponding diagram for the T-matrix of molecule-molecule scattering is shown in Fig. 5. We have $g_{\text{ind}} = \frac{4\pi\hbar^2 a_{\text{ind}}}{m_{\uparrow} + m_{\downarrow}} = T_m$ and:

$$T_m = g_r^4 \int \frac{d\omega}{2\pi} \int \frac{d^3\mathbf{p}}{(2\pi)^3} \frac{1}{(i\omega - \xi_{\mathbf{p}}^{\uparrow})^2} \frac{1}{(i\omega + \xi_{\mathbf{p}}^{\downarrow})^2} \quad (34)$$

where $g_r^2 = \frac{2\pi a_{bg} W}{m_r}$, $\xi_{\mathbf{p}}^{\sigma} = \frac{\mathbf{p}^2}{2m_{\sigma}} - \mu_{\sigma}$ and $\mu_{\downarrow} = E_m$ is given by the molecular energy in the single impurity problem. All the external frequency and momentums are set to zero.

After performing the frequency integral and some change of variables, we finally have:

$$k_F a_{\text{ind}} = \frac{1}{\pi} \gamma (1 + \gamma^{-1})^3 \left(k_F a_{bg} \frac{W}{\epsilon_F} \right)^2 F(\gamma, \frac{|E_m|}{\epsilon_F}) \quad (35)$$

$$F(\gamma, \eta) = 2 \int_1^{\infty} dx \frac{x^2}{[(1 + \gamma^{-1})x^2 + \eta - 1]^3} - \frac{1}{2(\gamma^{-1} + \eta)^2} \quad (36)$$

where $\gamma = \frac{m_{\downarrow}}{m_{\uparrow}}$.